

Comparison between Multi-Layer Perceptron and Radial Basis Function Networks for Sediment Load Estimation in a Tropical Watershed

Hadi Memarian¹, Siva Kumar Balasundram^{2*}

¹Department of Land Management, Faculty of Agriculture, Universiti Putra Malaysia, Serdang, Malaysia

²Department of Agriculture Technology, Faculty of Agriculture, Universiti Putra Malaysia, Serdang, Malaysia
Email: *siva@putra.upm.edu.my

Received August 21, 2012; revised September 20, 2012; accepted October 19, 2012

ABSTRACT

Prediction of highly non-linear behavior of suspended sediment flow in rivers has prime importance in environmental studies and watershed management. In this study, the predictive performance of two Artificial Neural Networks (ANNs), namely Radial Basis Function (RBF) and Multi-Layer Perceptron (MLP) were compared. Time series data of daily suspended sediment discharge and water discharge at the Langat River, Malaysia were used for training and testing the networks. Mean Square Error (MSE), Normalized Mean Square Error (NMSE) and correlation coefficient (r) were used for performance evaluation of the models. Using the testing data set, both models produced a similar level of robustness in sediment load simulation. The MLP network model showed a slightly better output than the RBF network model in predicting suspended sediment discharge, especially in the training process. However, both ANNs showed a weak robustness in estimating large magnitudes of sediment load.

Keywords: Sediment Load; Neural Network; MLP; RBF; Hulu Langat Watershed

1. Introduction

River suspended sediment load is a principal parameter in reservoir management and can serve as an index to understand the status of soil erosion and ecological environment in a watershed [1]. The rainfall-sediment yield process is extremely complex, non-linear, dynamic, and fragmented due to spatial variability of watershed geomorphologic characteristics, spatial/temporal variability of rainfall and involvement of other physical processes [2,3]. Therefore, predicting sediment yield process in river basins requires a non-linear modeling approach such as Artificial Neural Network (ANN), which can capture complex temporal variations within time series data [4].

The ANN is a powerful soft computational technique which has been widely used in many areas of water resource management and environmental sciences [5-15]. ANN comprises parallel systems that are composed of Processing Elements (PE) or neurons, which are assembled in layers and connected through several links or weights. After feeding input data to the input layer, they pass through and are operated on by the network until an output is produced at the output layer. Each neuron receives numerous inputs from other neurons through some

weighted connections. These weighted inputs are then summed and a standard threshold is added, generating the argument for a transfer function (usually linear, logistic, or hyperbolic tangent) which in turn produces the final output of the neuron [14].

This study was aimed at comparing the predictive performance of the Multi-Layer Perceptron (MLP) and the Radial Basis Function (RBF) neural networks in prediction of suspended sediment discharge at the Hulu Langat watershed using time series of daily water discharge as the input data.

2. Materials and Methods

2.1. Study Area

Hydrometeorologically, the Hulu Langat watershed is affected by two monsoon seasons, *i.e.* the Northeast (November to March) and the Southwest (May to September). Average annual rainfall is about 2400 mm. The wettest months are April and November with an average monthly rainfall exceeding 250 mm, while the driest month is June with an average monthly rainfall below 100 mm. Topographically, the Hulu Langat watershed can be divided into three distinct areas in reference to the Langat River, *i.e.* mountainous area in the upstream, un-

*Corresponding author.

dulating land in the center and flat flood plain in the downstream. This watershed consists of a rich diversity of landforms, surface features and land cover [16,17]. Descriptions about this watershed are shown in **Figure 1** and **Table 1**.

2.2. Data Sets

Daily water discharge and sediment load data from 1997 through 2008 recorded at Sungai Langat hydrometer station were obtained from the Department of Irrigation and Drainage (DID) of Malaysia.

2.3. Multi-Layer Perceptron

Multi-Layer Perceptron (MLP) is a popular architecture used in ANN. The MLP can be trained by a back-propagation algorithm [18]. Typically, the MLP is organized as a set of interconnected layers of artificial neurons, input, hidden and output layers. When a neural group is provided with data through the input layer, the neurons in this first layer propagate the weighted data and randomly selected bias through the hidden layers. Once the net sum at a hidden node is determined, an output response is provided at the node using a transfer function [19,20].

Two important characteristics of the MLP are its non-linear processing elements which have a non-linear acti-

vation function that must be smooth (the logistic function and the hyperbolic tangent are the most widely used) and its massive interconnectivity (*i.e.* any element of a given layer feeds all the elements of the next layer). The two main activation functions used in this study were sigmoid, and are described as follows:

$$\phi(y_i) = \tanh(w_i) \text{ and } \phi(y_i) = \left(1 + e^{-w_i}\right)^{-1} \quad (1)$$

in which the former function is a hyperbolic tangent ranging from -1 to 1 , and the latter is a logistic function similar in shape but ranges from 0 to 1 . Here, y_i is the output of the i th node (neuron) and w_i is the weighted sum of the input synapses [15,21,22].

The MLP network is trained with error correction learning, which means that the desired response for the system must be known. Error correction learning works in the following way: From the system response at PE_i at iteration n , $y_i(n)$ and the desired response $d_i(n)$ for a given input pattern, an instantaneous error $e_i(n)$ is defined by:

$$e_i(n) = d_i(n) - y_i(n) \quad (2)$$

Using the theory of gradient descent learning [21, 23-25], each weight in the network can be adapted by correcting the present value of the weight with a term that is proportional to the present input and error at the weight, such that:

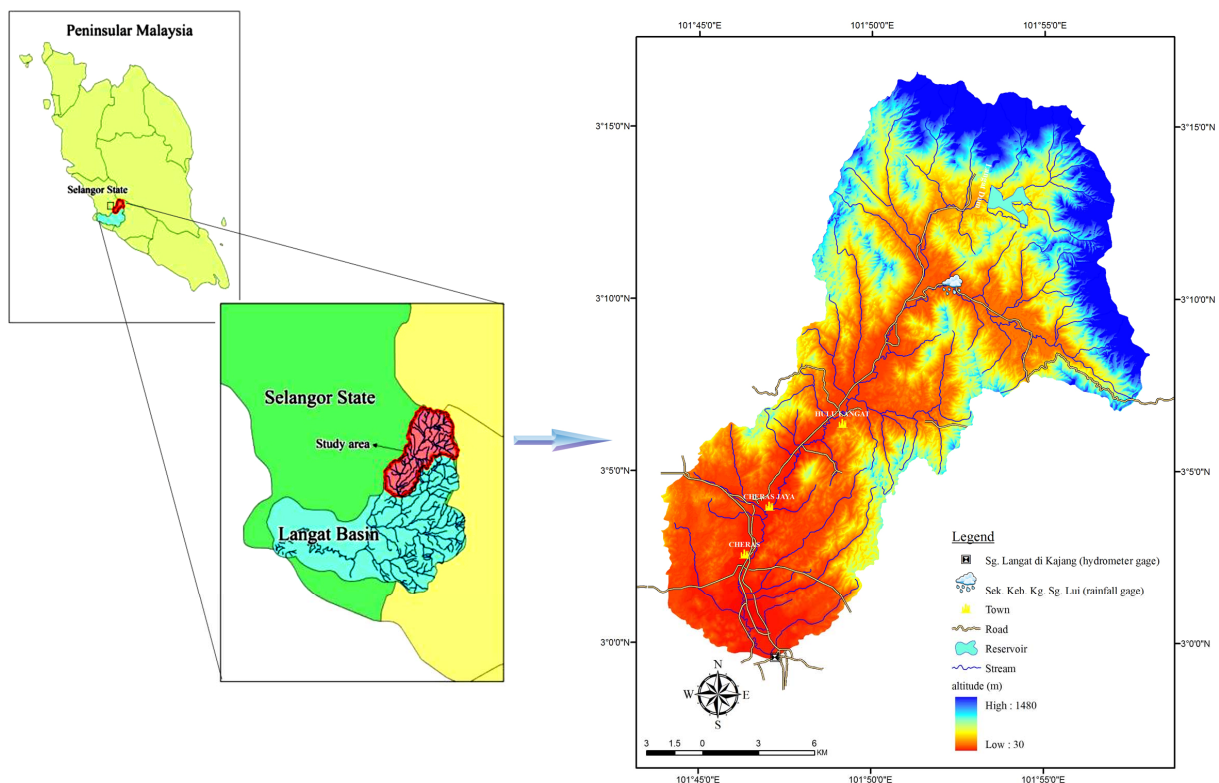


Figure 1. Location of study area.

Table 1. General information of the Hulu Langat watershed.

Main River	Langat
Geographic Coordinate	3°00' - 3°17'N and 101°44' - 101°58'E
Drainage Area (km ²)	390.26
Watershed Length (km)	34.5
Average Slope (%)	29.5
Max. Altitude (m)	1480
Min. Altitude (m)	36
Ave. Altitude (m)	278
Reference Hydrometer Station	Sungai Langat
Annual Water Discharge (*10 ⁶ m ³)	289.64
Annual Sediment Load (*10 ³ ton)	146.6
Annual Runoff (mm·km ⁻²)	742.16
Annual Sediment Yield (ton·km ⁻²)	375.65
Reference Rainfall Station	UPM Serdang, Kampung Lui, Ladang Dominion
Precipitation (mm)	2453
Land Cover*	Forest (54.6%), Cultivated Rubber (15.6%), Orchard (2%), Urbanized Area (15%), Horticulture and Crops, Oil Palm, Lake and Mining Land (12.8%)

*Based on the 2006 land use map.

$$w_{ij}(n+1) = w_{ij}(n) + \eta \delta_i(n) x_j(n) + \alpha (w_{ij}(n) - w_{ij}(n-1)) \quad (3)$$

The local error $\delta_i(n)$ can be directly computed from $e_i(n)$ at the output PE or can be computed as a weighted sum of errors at the internal PEs. The constant η is known as the step size and α is known as the momentum. This procedure is referred to as the back-propagation algorithm imposed into the momentum learning. Back-propagation computes the sensitivity of a cost function with respect to each weight in the network, and updates each weight proportional to the sensitivity [21,24].

2.4. Radial Basis Function

The Radial Basis Function (RBF) is another popular architecture used in ANN. The RBF, which is multilayer and feed-forward, is often used for strict interpolation in multi-dimensional space. The term “feed-forward” means that the neurons are organized as layers in a layered neural network [26]. The basic architecture of a three-layered neural network is shown in **Figure 2**.

The RBF network comprises three layers, *i.e.* input, hidden and output. The input layer is composed of input data. The hidden layer transforms the data from the input space to the hidden space using a non-linear function. The output layer, which is linear, yields the response of

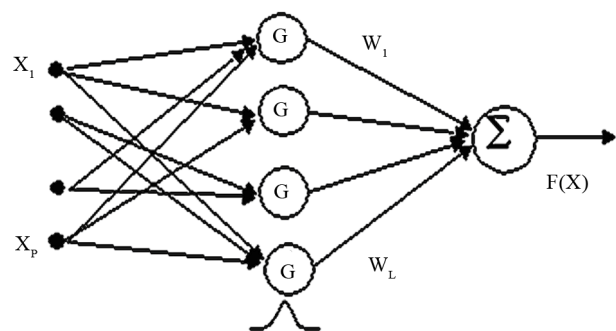
the network. The argument of the activation function of each hidden unit in an RBF network computes the Euclidean distance between the input vector and the center of that unit. In the structure of RBF network, the input data, x , is a p -dimensional vector, which is transmitted to each hidden unit. The activation function of hidden units is symmetric in the input space, and the output of each hidden unit depends only on the radial distance between the input vector, x , and the center for the hidden unit [26]. Each node in the hidden layer is a p -multivariate Gaussian function, given as follows:

$$G(x', x_i) = \exp \left[\frac{-1}{2\sigma_i^2} \sum_{k=1}^p (x_k - x_{ik})^2 \right] \quad (4)$$

where: x_i is the mean (center) and σ_i is the variance (width). These functions are referred to as radial basis functions. Finally, a linear weight is applied to the output of the hidden nodes to obtain:

$$F(x) = \sum_{i=1}^N w_i (G(x', x_i)) \quad (5)$$

The problem with this solution is that it may lead to a very large hidden layer. Thus, the solution should be approximated to reduce the number of PEs in the hidden layer and cleverly position them over the input space regions. This entails the need to estimate the position of each radial basis function and its variance, as well as to compute the linear weights, w_i [21,26]. An unsupervised technique, known as the k -nearest neighbor rule, is used to estimate the mean and the variance. The input space is first discretized into k clusters and the size of each cluster is obtained from the structure of the input data. The centers of the clusters give the centers of the RBFs, while the distance between the clusters provides the width of the Gaussians. NeuroSolutions, an ANN computer program, uses competitive learning to compute the centers and the widths. It sets each width proportional to the distance between the center and its nearest neighbor. The output weights are obtained through supervised learning. Therefore, the error correction learning described earlier in the MLP section is employed [21,27].

**Figure 2. Basic RBF architecture.**

2.5. Performance Metrics

The metrics used for network training and validation were Mean Square Error (MSE), Normalized Mean Square Error (NMSE) and correlation coefficient (r). Meanwhile, Akaike's Information Criterion (AIC) and Minimum Description Length (MDL) measurements were used by NeuroSolutions to produce a network with the best generalization. The AIC is used to measure the tradeoff between training performance and network size. The MDL is similar to the AIC in that it tries to combine the model's error with the number of degrees of freedom to determine the level of generalization [21,24]. The computations of MSE, NMSE and r are given below:

$$\text{MSE} = \frac{\sum_{j=0}^P \sum_{i=0}^N (d_{ij} - y_{ij})^2}{NP} \quad (6)$$

$$\text{NMSE} = \frac{P N \text{MSE}}{\sum_{j=0}^P \frac{N \sum_{i=0}^N d_{ij}^2 - \left(\sum_{i=0}^N d_{ij}\right)^2}{N}} \quad (7)$$

$$r = \frac{\sum_i (x_i - \bar{x})(d_i - \bar{d})}{\sqrt{\sum_i (d_i - \bar{d})^2} \sqrt{\sum_i (x_i - \bar{x})^2}} \quad (8)$$

where: P is the number of output processing elements, N is the number of exemplars in the data set, y_{ij} is network output for the exemplar i at the processing element j , and d_{ij} is desired output for the exemplar i at the processing element j [21,24].

2.6. Application of MLP

Data randomization was performed before the training process. In the training process, 54% and 14% of the total data were utilized for training and cross validation, respectively. Network testing was conducted using 32% of the total data. Data normalization was performed using NeuroSolutions. In this process, data sets were scaled in the range of 0.05 - 0.95. The number of neurons in the first and second hidden layers, and learning rates were determined based on several trials. The optimum properties of the MLP network are shown in **Table 2**.

2.7. Application of RBF

Network training and testing were performed using the same data sets applied in the MLP network. With regard to the form of activation function, applied in the hidden layer (*i.e.* hyperbolic tangent), data sets were normalized in the scale of -0.9 - 0.9. The number of neurons in the hidden layer, the number of clusters and learning rates were determined based on several trials. The optimum properties of the RBF network are shown in **Table 2**.

3. Results and Discussion

3.1. Error Analysis during the Training Process

Minimum MSE and final MSE obtained during the training process of the RBF network were significantly larger than those in the MLP network (**Table 3** and **Figure 3**). Comparatively, the MLP network is able to produce a more fitted output to cross validation data set in comparison to the RBF network. As indicated in recent literature [4,28], the RBF network gives a higher performance than the MLP network when the input data is multi dimensional. In this work, only water discharge was used as the input data. Thus, higher performance of the MLP network as compared to the RBF network is justifiable, especially during the training process.

3.2. Error Analysis during the Testing Process

Based on **Table 4**, both ANNs show similar strength in sediment load simulation during the testing process. However, application of the MLP network using the testing data set resulted in lesser MSE and NMSE, as compared to the RBF network. Difference in the r value between both networks is negligible.

Table 2. Optimum properties of the ANNs.

Network properties	ANN	
	MLP	RBF
Number of hidden layers	2	1
Number of neurons in the first hidden layer	20	20
Number of neurons in the second hidden layer	10	-
Momentum rate & step size in the first hidden layer	0.7 & 1.0	0.7 & 1.0
Momentum rate & step size in the second hidden layer	0.7 & 0.1	-
Momentum rate & step size in the output layer	0.7 & 0.01	0.7 & 0.1
Activation function in the first hidden layer	Logistic	Hyperbolic tangent
Activation function in the second hidden layer	Logistic	-
Activation function in the output layer	Linear logistic	Bias
Number of cluster centers in the input layer	-	5
Number of epochs for supervised learning	1200	1000
Number of epochs for unsupervised learning	-	100
Number of exemplars for training	1795	1795
Number of exemplars for cross validation	450	450
Number of exemplars for testing	1058	1058

Table 3. Error analysis during the training process.

Best Networks	MLP		RBF	
	Training	Cross Validation	Training	Cross Validation
Epoch [#]	1200	820	999	584
Minimum MSE	0.001598738	0.001605163	0.006131928	0.006382225
Final MSE	0.001598738	0.001613058	0.006131928	0.006416793

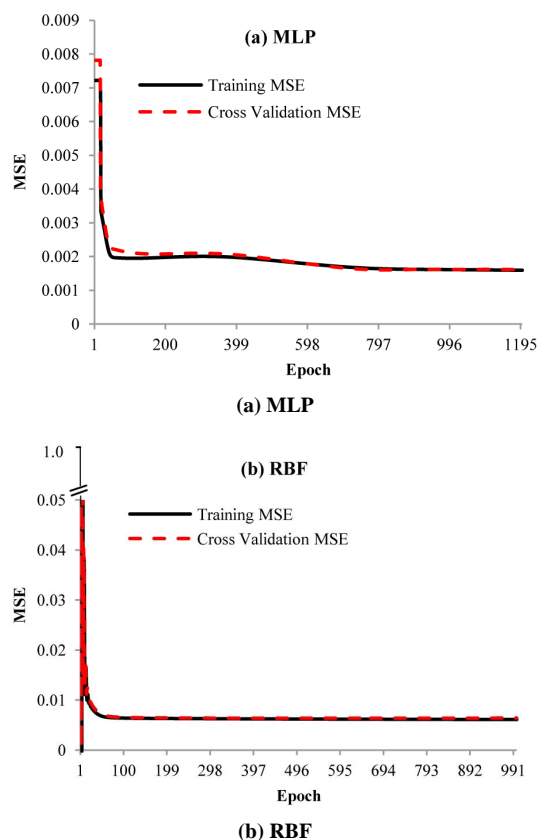


Figure 3. MSE versus epoch for (a) MLP and (b) RBF.

Table 4. Performance metrics computed based on the testing data set.

Performance	MLP	RBF
MSE	274088.998	281938.375
NMSE	0.420	0.432
MAE	131.454	130.925
Min Abs Error	0.069	0.186
Max Abs Error	6823.613	6838.253
r	0.812	0.814

The MLP network is comparatively more capable of tracing fluctuations in daily sediment load than the RBF network (Figures 4 and 5). As highlighted in Figures 4 and 5, the points corresponding to sediment load with an observed large magnitude are mostly situated at the bottom quad of the 1:1 line. Clearly, both ANNs showed weak robustness in estimating sediment load with a large magnitude, especially for records higher than 4000 ton/day. Such limitation in the application of neural networks has also been reported in the works of Hsu *et al.* (1995) [29], Morid *et al.* (2002) [30] and Talebizadeh *et al.* (2010) [14], commonly attributable to scarcity of large observed values in the training data set. In other words, inefficiency of the ANN model in estimating large magnitudes of sediment load can be attributed to different non-linear relationships governing the process of sediment detachment and final sediment load generated from a watershed. For example, the mechanism of sediment load generation induced by a low flow event is obviously different from the sediment load produced by a storm event in which a significant amount of wash load enters the watershed drainage network and passes the outlet. Therefore, due to different mechanisms, a single ANN which may produce satisfactory results for the simulation of medium and low loads may not simulate large sediment load events with the same accuracy. In this data set, there was inadequate data corresponding to high sediment load events to train a separate ANN model for simulating these high values, as suggested by Cigizoglu and Kisi (2006) [31] and confirmed by Talebizadeh *et al.* (2010) [14].

Besides the above reason, in recent decades, the Hulu Langat watershed has experienced an extensive rate of urban development. Infrastructure constructions such as roads, tunnels, and bridges, and landslide occurrences can result in large amounts of sediment load for a number of years which can affect water quantity and quality. Wastewater discharges into water streams from industrial or residential areas and water treatment plants are mostly

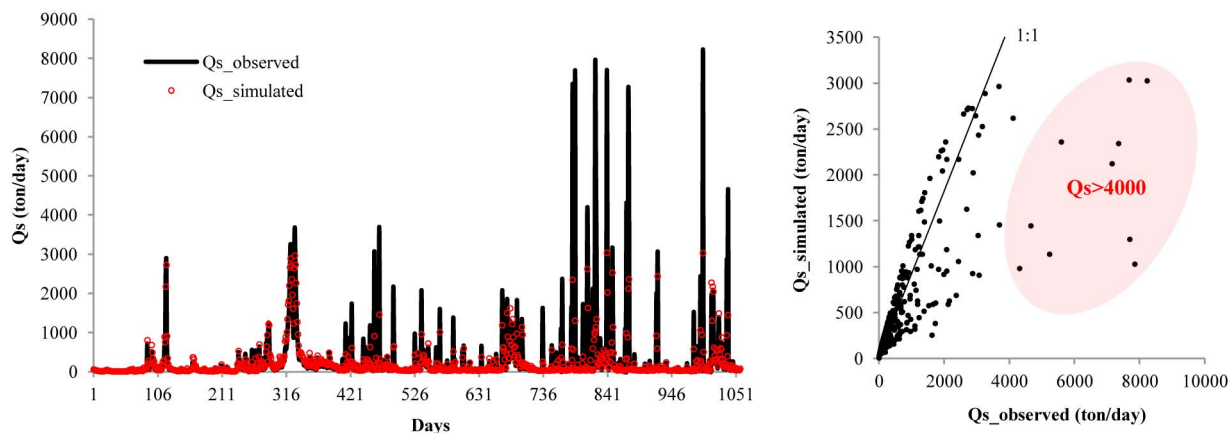


Figure 4. Observed sediment load versus simulated sediment load by the MLP network.

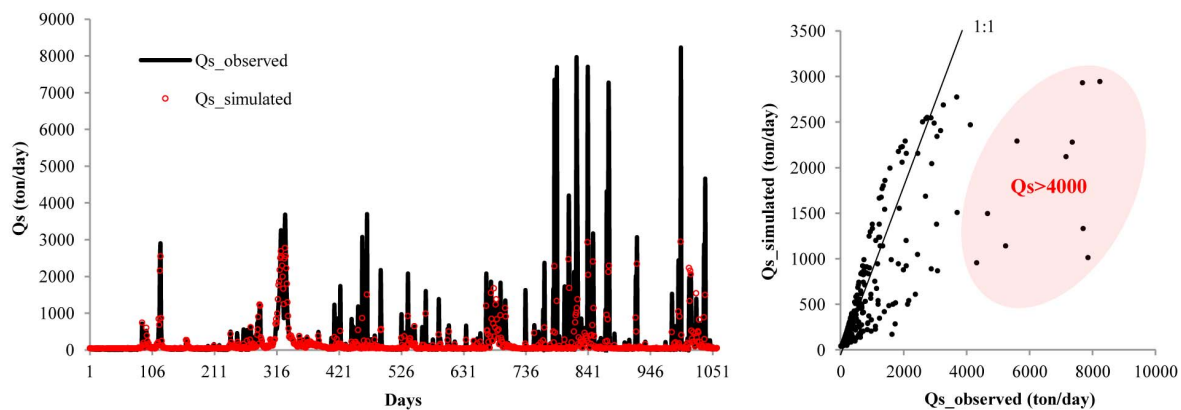


Figure 5. Observed sediment load versus simulated sediment load by the RBF network.

unknown in the Hulu Langat watershed. These sources of sediment load are not describable only by water discharge and can produce a large amount of uncertainty in ANN simulation [32,33]. Therefore, using more input data (e.g. rainfall, temperature and reservoir level) would assist us in obtaining a higher level of accuracy for sediment load simulation by ANN.

4. Conclusion

The minimum MSE obtained during the training process of the RBF network was significantly larger than that in the MLP network. Thus, the MLP network produced a more fitted output to the cross validation data set than the RBF network. Network testing showed that both ANNs had similar strength in sediment load simulation. However, the application of the MLP network using the testing data set resulted in lesser amounts of the MSE and NMSE, *i.e.* 274,089 and 0.42, respectively, as compared to the RBF network. In addition, the MLP network was more capable in tracing fluctuations in daily sediment load than the RBF network. Both ANNs showed a weak robustness in estimating large magnitudes of sediment load, especially for records higher than 4000 ton/day. This was attributable to scarcity of large observed values in the training data set and different non-linear relationships governing the process of sediment detachment and final sediment load by a high storm event, as compared to those by low or medium storm events. Additionally, infrastructure constructions, landslide occurrences and wastewater discharges in the study area resulted in large amounts of sediment load over several years, which affected water quantity and quality. These sources of sediment load may have contributed to a level of uncertainty in ANN simulation.

5. Acknowledgements

Necessary hydrological data for this study was provided

by the Department of Irrigation and Drainage, Malaysia.

REFERENCES

- [1] C. Chutachindakate and T. Sumi, "Sediment Yield and Transportation Analysis: Case Study on Managawa River Basin," *Annual Journal of Hydraulic Engineering*, Vol. 52, 2008, pp. 157-162.
- [2] B. Zhang and R. S. Govindaraju, "Geomorphology-Based Artificial Neural Networks (GANNs) for Estimation of Direct Runoff over Watersheds," *Journal of Hydrology*, Vol. 273, No. 1-4, 2003, pp. 18-34. [doi.10.1016/S0022-1694\(02\)00313-X](https://doi.org/10.1016/S0022-1694(02)00313-X)
- [3] G. Singh and R. K. Panda, "Daily Sediment Yield Modeling with Artificial Neural Network Using 10-Fold cross Validation Method: A Small Agricultural Watershed, Kapgari, India," *International Journal of Earth Sciences and Engineering*, Vol. 4, No. 6, 2011, pp. 443-450.
- [4] M. R. Mustafa, M. H. Isa and R. B. Rezaaur, "A Comparison of Artificial Neural Networks for Prediction of Suspended Sediment Discharge in River—A Case Study in Malaysia," *World Academy of Science, Engineering and Technology*, Vol. 81, 2011, pp. 372-376.
- [5] H. Halff, M. H. Halff and M. Azmoodeh, "Predicting Runoff from Rainfall Using Neural Networks," *Proceedings of the Engineering and Hydrology*, New York, 1993, pp. 760-765.
- [6] N. Karunithi, W. J. Grenney, D. Whitley and K. Bovee, "Neural Networks for River Flow Prediction," *Journal of Computing in Civil Engineering*, Vol. 8, 1994, pp. 201-220.
- [7] J. Smith and R. N. Eli, "Neural Network Models of Rainfall Runoff Process," *Journal of Water Resources Planning and Management*, Vol. 121, No. 6, 1995, pp. 499-580. [doi.10.1061/\(ASCE\)0733-9496\(1995\)121:6\(499\)](https://doi.org/10.1061/(ASCE)0733-9496(1995)121:6(499))
- [8] D. F. Lekkas, C. Onof, M. J. Lee and E. A. Baltas, "Application of Artificial Neural Networks for Flood Forecasting," *Global Nest: The International Journal*, Vol. 6, No. 3, 2004, pp. 205-211.
- [9] K. Cigizoglu and M. Alp, "Rainfall-Runoff Modelling Using Three Neural Network Methods," In: L. Rutkowski,

- J. Siekmann, R. Tadeusiewicz and L. A. Zadeh, Eds., *Artificial Intelligence and Soft Computing—ICAISC 2004*, Springer, Berlin, Heidelberg, Vol. 3070, 2004, pp. 166-171.
- [10] H. K. Cigizoglu, "Estimation and Forecasting of Daily Suspended Sediment Data by Multi-Layer Perceptrons," *Advances in Water Resources*, Vol. 27, No. 2, 2004, pp. 185-195. [doi.10.1016/j.advwatres.2003.10.003](https://doi.org/10.1016/j.advwatres.2003.10.003)
- [11] S. S. Eslamian, S. A. Gohari, M. Biabanaki and R. Malekian, "Estimation of Monthly Pan Evaporation Using Artificial Neural Networks and Support Vector Machines," *Journal of Applied Sciences*, Vol. 8, No. 19, 2008, pp. 3497-3502.
- [12] V. Jothiprakash and V. Garg, "Reservoir Sedimentation Estimation Using Artificial Neural Network," *Journal of Hydrologic Engineering*, Vol. 14, 2009, pp. 1035-1040. [doi.10.1061/\(ASCE\)HE.1943-5584.0000075](https://doi.org/10.1061/(ASCE)HE.1943-5584.0000075)
- [13] H. Memarian, S. Feiznia and S. Zakikhani, "Estimating River Suspended Sediment Yield Using MLP Neural Network in Arid and Semi-Arid Basins, Case Study: Bar river, Neyshaboor, Iran," *Desert*, Vol. 14, 2009, pp. 43-52.
- [14] M. Talebizadeh, S. Morid, S. A. Ayyoubzadeh and M. Ghasemzadeh, "Uncertainty Analysis in Sediment Load Modeling Using ANN and SWAT Model," *Water Resources Management*, Vol. 24, No. 9, 2010, pp. 1747-1761. [doi.10.1007/s11269-009-9522-2](https://doi.org/10.1007/s11269-009-9522-2)
- [15] A. Singh, M. Imtiyaz, R. K. Isaacs and D. M. Denisc, "Comparison of Soil and Water Assessment Tool (SWAT) and Multilayer Perceptron (MLP) Artificial Neural Network for Predicting Sediment Yield in the Nagwa Agricultural Watershed in Jharkhand, India," *Agricultural Water Management*, Vol. 104, 2012, pp. 113-120. [doi.10.1016/j.agwat.2011.12.005](https://doi.org/10.1016/j.agwat.2011.12.005)
- [16] H. Memarian, S. K. Balasundram, J. Talib, C. B. S. Teh, M. S. Alias, K. C. Abbaspour and A. Haghizadeh, "Hydrologic Analysis of a Tropical Watershed Using KINEROS 2," *Environment Asia*, Vol. 5, No. 1, 2012, pp. 84-93.
- [17] H. Memarian, S. K. Balasundram, J. Talib, M. S. Alias and K. C. Abbaspour, "Trend Analysis of Water Discharge and Sediment Load during the Past Three Decades of Development in the Langat Basin, Malaysia," *Hydrological Sciences Journal*, Vol. 57, No. 6, 2012, pp. 1207-1222. [doi.10.1080/02626667.2012.695073](https://doi.org/10.1080/02626667.2012.695073)
- [18] E. Rumelhart, J. L. McClelland and the PDP Research Group, "Parallel Distributed Processing: Explorations in the Microstructure of Cognition, Vol. 1: Foundations," MIT Press, Cambridge, 1986.
- [19] J. T. Kuo, M. H. Hsieh, W. S. Lung and N. She, "Using Artificial Neural Network for Reservoir Entrophication Prediction," *Ecological Modelling*, Vol. 200, No. 1-2, 2007, pp. 171-177. [doi.10.1016/j.ecolmodel.2006.06.018](https://doi.org/10.1016/j.ecolmodel.2006.06.018)
- [20] M. Kim and J. E. Gilley, "Artificial Neural Network Estimation of Soil Erosion and Nutrient Concentrations in Runoff from Land Application Areas," *Computers and Electronics in Agriculture*, Vol. 64, No. 2, 2008, pp. 268-275. [doi.10.1016/j.compag.2008.05.021](https://doi.org/10.1016/j.compag.2008.05.021)
- [21] J. C. Principe, W. C. Lefebvre, G. Lynn, C. Fancourt and D. Wooten, "NeuroSolutions-Dokumentation, the Manual and On-Line Help," 2007.
- [22] T. Rajaei, S. A. Mirbagheri, M. Zounemat-Kermani and V. Nourani, "Daily Suspended Sediment Concentration Simulation Using ANN and Neuro-Fuzzy Models," *Science of the Total Environment*, Vol. 407, No. 17, 2009, pp. 4916-4927. [doi.10.1016/j.scitotenv.2009.05.016](https://doi.org/10.1016/j.scitotenv.2009.05.016)
- [23] P. Baldi, "Gradient Descent Learning Algorithm Overview: A General Dynamical Systems Perspective," *IEEE Transactions on Neural Networks*, Vol. 6, No. 1, 1995, pp. 182-195.
- [24] J. C. Principe, N. R. Euliano and W. C. Lefebvre, "Neural and Adaptive Systems: Fundamentals through Simulations," John Wiley & Sons Inc., Hoboken, 2000.
- [25] D. Graupe, "Principles of Artificial Neural Networks (2nd Edition), Advanced Series on Circuits and Systems," Vol. 6, World Scientific Publishing, Singapore City, 2007.
- [26] F. Lin and L. H. Chen, "A Non-Linear Rainfall-Runoff Model Using Radial Basis Function Network," *Journal of Hydrology*, Vol. 289, No. 1-4, 2004, pp. 1-8. [doi.10.1016/j.jhydrol.2003.10.015](https://doi.org/10.1016/j.jhydrol.2003.10.015)
- [27] M. T. Musavi, W. Ahmed, K. H. Chan, K. B. Faris and D. M. Hummels, "On the Training of Radial Basis Function Classifiers," *Neural Network*, Vol. 5, No. 4, 1992, pp. 595-603. [doi.10.1016/S0893-6080\(05\)80038-3](https://doi.org/10.1016/S0893-6080(05)80038-3)
- [28] M. Alp and H. K. Cigizoglu, "Suspended Sediment Load Simulation by Two Artificial Neural Network Methods Using Hydrometeorological Data," *Environmental Modelling and Software*, Vol. 22, No. 1, 2007, pp. 2-13. [doi.10.1016/j.envsoft.2005.09.009](https://doi.org/10.1016/j.envsoft.2005.09.009)
- [29] K. L. Hsu, H. Gupta and S. Sorooshian, "Artificial Neural Network Modeling of the Rainfall Runoff Process," *Water Resources Research*, Vol. 31, No. 10, 1995, pp. 2517-2530. [doi.10.1029/95WR01955](https://doi.org/10.1029/95WR01955)
- [30] S. Morid, A. K. Gosain and A. K. Keshari, "Solar Radiation Estimation Using Temperature-Based, Stochastic and Artificial Neural Networks Approaches," *Nordic Hydrology*, Vol. 3, No. 4, 2002, pp. 291-304. [doi.10.2166/nh.2002.017](https://doi.org/10.2166/nh.2002.017)
- [31] H. K. Cigizoglu and O. Kisi, "Methods to Improve the Neural Network Performance in Suspended Sediment Estimation," *Journal of Hydrology*, Vol. 317, No. 3-4, 2006, pp. 221-238. [doi.10.1016/j.jhydrol.2005.05.019](https://doi.org/10.1016/j.jhydrol.2005.05.019)
- [32] K. C. Abbaspour, "User Manual for SWAT-CUP4, SWAT Calibration and Uncertainty Analysis Programs," Swiss Federal Institute of Aquatic Science and Technology, Dübendorf, 2011.
- [33] C. Jones, M. Sultan, E. Yan, A. Milewski, M. Hussein, A. Al-Dousari, S. Al-Kaisy and R. Becker, "Hydrologic Impacts of Engineering Projects on the Tigris-Euphrates System and Its Marshlands," *Journal of Hydrology*, Vol. 353, No. 1-2, 2008, pp. 59-75. [doi.10.1016/j.jhydrol.2008.01.029](https://doi.org/10.1016/j.jhydrol.2008.01.029)